The International Archives of the Photogrammetry, Remote Sensing and Spatial Information Sciences, Volume XLVIII-G-2025
ISPRS Geospatial Week 2025 "Photogrammetry & Remote Sensing for a Better Tomorrow…", 6–11 April 2025, Dubai, UAE

Seasonal Changes in the Health of Mangroves in Abu Dhabi Over 10 years Using Landsat Data

Shahira Abdul Lathif[1], Alfiya Fathima Paradan[1], Batoul Mohsen[1], Shabniya Veliyampatt[1], and Maryam R. Al Shehhi[1]

[1] Department of Civil and Environmental Engineering, Khalifa University, Abu Dhabi, UAE
(100061032,100060968,100062019,100061982,maryamr.alshehhi)@ku.ac.ae

Keywords: Mangroves, Mangrove Health Index, Temperature, Combined Mangrove Recognition Index, Arabian Gulf, Landsat

Abstract

Mangrove ecosystems play a crucial role in coastal protection, biodiversity conservation, and climate regulation. Using satellite imagery, this study examines the seasonal changes in mangrove health in Abu Dhabi over the years 2013 to 2021. Landsat 8 data were analyzed to assess mangrove extent and condition, focusing on vegetation indices and land surface temperature to understand their response to environmental factors. Results indicate that mangrove health fluctuates with seasonal temperature variations, with vegetation indices ranging from 0.3 in summer to above 0.6 in winter. The highest values were recorded in December, indicating peak health, while August exhibited the lowest, reflecting stress from extreme temperatures exceeding 40°C. A strong negative correlation (-0.75) was observed between vegetation health and surface temperature, confirming that elevated temperatures reduce mangrove vitality. Over the study period, mangrove cover increased by approximately 12%, highlighting the success of conservation initiatives. This study underscores the importance of continuous monitoring for conservation planning and climate adaptation. Satellite-based assessments provide valuable insights into mangrove ecosystem dynamics, advocating for targeted preservation measures.

1. Introduction

Mangrove forests are essential coastal ecosystems that serve as natural buffers against shoreline erosion, provide habitats for diverse marine species, and contribute to carbon sequestration (Gandhi and Jones, 2019, Nyanga, 2020, Al Shehhi and Kaya, 2021). These ecosystems also play a crucial role in stabilizing coastlines by reducing wave energy and preventing coastal degradation, making them indispensable for protecting coastal communities. In the United Arab Emirates (UAE), mangroves are an integral part of the coastal landscape, particularly in Abu Dhabi, which hosts approximately 10,834 hectares of mangrove forests, making up a significant portion of the country's total mangrove cover (Amrousi et al., 2024). These ecosystems serve as a key component of the region's biodiversity, supporting marine food webs and providing breeding grounds for various fish species and other aquatic organisms. The dominant species, Avicennia marina, thrives in arid coasts, tolerating high salinity and extreme temperatures, making it vital to these environments. It possesses unique physiological adaptations such as salt-excreting leaves and aerial roots, allowing it to survive in harsh intertidal zones (Yousif and Sen, 2020). Despite their ecological importance, mangroves in Abu Dhabi face multiple environmental and anthropogenic threats, including extreme temperatures, habitat degradation, and climate change (Paleologos et al., 2019, Al Shehhi et al., 2017, Shehhi et al., 2020). The region experiences harsh climatic conditions, with summer temperatures reaching up to 47^oC, minimal rainfall of less than 40 mm per year, and high coastal salinity levels of 40 g/kg. These factors collectively challenge mangrove survival and regeneration, making conservation efforts imperative. Additionally, rising temperatures and shifting precipitation patterns exacerbate ecosystem vulnerability, affecting mangrove productivity and potentially altering their spatial distribution over time (Al-Shehhi et al., 2021). Further, urban expansion and coastal development have led to habitat fragmentation, disrupting natural mangrove dynamics and reducing their overall resilience (Alongi, 2015). The encroachment of infrastructure projects and dredging activities further threaten their existence, leading to increased sedimentation and changes in hydrological regimes that negatively impact seedling establishment and growth (Godoy and Lacerda, 2015).

Conventional field-based assessments of mangroves are often strenuous, costly, and logistically challenging, particularly due to the remoteness of many mangrove-rich locations. These limitations necessitate the adoption of remote sensing technologies, which provide a cost-effective, large-scale, and non-intrusive means to monitor mangrove health (Asmara et al., 2021). Satellite imagery allows researchers to track spatial extent, assess vegetation condition, and evaluate thermal stress, offering critical insights into mangrove dynamics. Moreover, remote sensing techniques enable frequent and systematic observations, facilitating the assessment of long-term trends and guiding conservation strategies (Pham et al., 2019). By incorporating remote sensing, a more comprehensive approach can be developed to assess the impacts of both natural and anthropogenic pressures on mangrove ecosystems (Lathif and Al Shehhi, 2025).

Various spectral indices have been developed to study mangrove health, among which the Normalized Difference Vegetation Index (NDVI) and the Combined Mangrove Recognition Index (CMRI) are widely used. NDVI is an effective tool for evaluating vegetation health, with higher values indicating healthy, dense vegetation and lower values signaling stressed or degraded areas (Bukowiecki et al., 2020). CMRI enhances mangrove classification by integrating multiple spectral features, improving the ability to distinguish mangroves from other vegetation types (Gupta et al., 2018). Additionally, indices like the Normalized Difference Moisture Index (NDMI) assess water content, while the Soil Adjusted Vegetation Index (SAVI) accounts for soil brightness variations, providing complementary insights into mangrove health and distribution (Baloloy et al., 2020, Faridah-Hanum et al., 2019). Moreover, land surface temperature analysis helps assess the impact of thermal stress on mangrove ecosystems, offering insights into the relationship between vegetation health and temperature fluctuations. The integration of these indices allows for a multi-faceted evaluation of mangrove conditions, improving the accuracy of health assessments.

This study aims to leverage remote sensing techniques to: (1) quantify the changes in mangrove extent in Abu Dhabi between 2013 and 2021, (2) evaluate seasonal variations in mangrove health using vegetation indices, (3) analyze temperature-induced stress using land surface temperature data, and (4) determine the relationship between temperature fluctuations and vegetation indices. By integrating multi-year satellite data and advanced remote sensing techniques, this research provides a comprehensive understanding of mangrove ecosystem dynamics, supporting the development of conservation strategies to ensure their long-term sustainability. The findings from this study will contribute to the broader discourse on climate adaptation and coastal ecosystem resilience, offering valuable insights for policymakers, conservationists, and environmental researchers. As the impacts of climate change intensify, understanding the interactions between mangroves, temperature variations, and conservation efforts will be essential in shaping effective policies for the sustainable management of coastal ecosystems (Osland et al., 2018, Worthington et al., 2020). Furthermore, the results can help refine remote sensing methodologies for future environmental monitoring, ensuring that mangrove ecosystems continue to thrive in the face of environmental challenges.

2. Methodology

2.1 Study Area

The study area lies between $24^o26'08" N$ and $24^o42'08" N$ and between $54^o23'17" E$ and $54^o39'17" E$ (Figure 1). Mangroves in Abu Dhabi extend from the east to the west of the city, however this study focuses on the Eastern and Jubail areas where the highest concentration of mangroves can be observed. A total of 378.05 km^2 of land is covered by this study area, which stretches from Mussaffah in the southwest to Al Weheil Island in the northeast. This study region is characterized by flat, salt-encrusted soil, a thin layer of blue-green algae, mangroves, seagrass, sabkha, terrestrial vegetation, and open lands (Elmahdy and Mohamed, 2013). This region is located within an arid climate zone and averages temperatures of 47^oC in the summer and 12^oC in the winter and has a mean annual rainfall of less than 40 mm and an evaporation rate of 124 cm per year (Al-Shehhi et al., 2021, Gafoor et al., 2025).

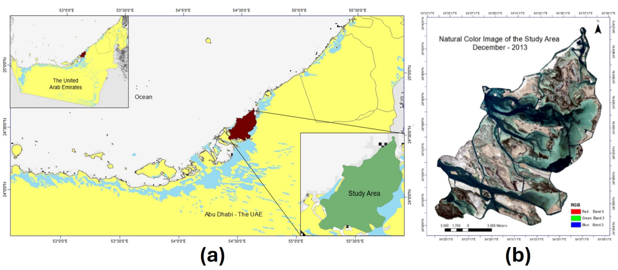

Figure 1. (a) The study area encompasses the major mangrove habitats along the coastal line of Abu Dhabi and (b) RGB true color image of the mangroves' region

2.2 Satellite Images Retrievals and Processing

This study utilized Landsat 8 Operational Land Imager (OLI) and Thermal Infrared Sensor (TIRS) multispectral imagery to analyze the region of interest. Landsat 8, operating under the Worldwide Reference System-2, captures images every 16 days, enabling temporal assessments (Pagkalinawan, 2015). To ensure seasonal variability, 36 images from 2013 to 2021 were selected, covering April, August, and December annually (Table 1). Preprocessing involved three key steps: conversion to Top of Atmosphere (TOA) Reflectance with scattering corrections and sun-angle normalization, TOA Brightness Temperature derivation for thermal analysis, and Land Surface Temperature (LST) estimation using the radiometrically calibrated thermal band. The details of these conversions are described in sections 2.2.1 and 2.2.2. Furthermore, the QGIS Semiautomatic Classification (SAC) plugin (Congedo, 2021) was employed for radiometric calibration, region extraction, mapping, and LST estimation, ensuring accurate spectral and thermal assessments (Figure 2).

Parameters	Description of Landsat 8 OLI
Acquisition Date	For the months of April, August, and December starting from 2013 to 2021
Path	160
Raw	43
Bands Utilized	Band 2, Band 3, Band 4, Band 5, Band 10

Table 1. Details of the Satellite Data Used

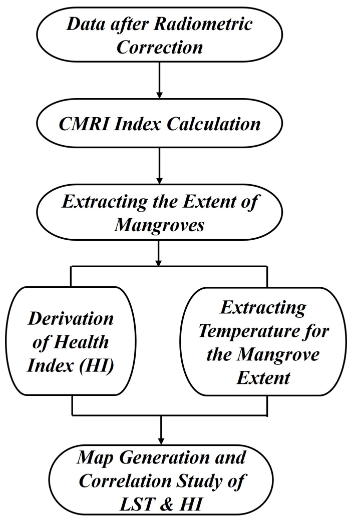

Figure 2. Flow chart summarizing the main methods implemented in this work

2.2.1 TOA Reflectance

To standardize the satellite imagery, digital number (DN) values were converted into TOA spectral radiance using radiometric rescaling factors provided in the metadata (Using the USGS Landsat Level-1 Data Product | U.S. Geological Survey, 2024). This process ensures consistency in reflectance values by adjusting for sensor-specific calibration factors. The conversion to TOA planetary reflectance was performed without sun angle correction using the equation 1:

$$\rho_\lambda{}' = M_\rho Q_{cal} + A_\rho \qquad (1)$$

where $\rho_\lambda{}'$ represents TOA planetary reflectance before sun angle correction, M_ρ is the band-specific multiplicative rescaling factor, A_ρ is the additive rescaling factor, and Q_{cal} corresponds to the calibrated pixel values (DN). To account for solar illumination variations, sun angle correction was applied using equation 2:

$$\rho_\lambda = \frac{\rho_\lambda{}'}{\cos(\theta_{SZ})} = \frac{\rho_\lambda{}'}{\sin(\theta_{SE})} \tag{2}$$

where ρ_λ is the TOA planetary reflectance, θ_{SE} is the local sun elevation angle, and θ_{SZ} is the local solar zenith angle, calculated as $\theta_{SZ} = 90^\circ - \theta_{SE}$.

2.2.2 TOA Brightness Temperature (TOA BT) The TOA BT was derived from the TOA spectral radiance to assess thermal emissions from the Earth's surface (Equation 3) (Using the USGS Landsat Level-1 Data Product | U.S. Geological Survey, 2024).

$$T = \frac{K_2}{\ln\left(\frac{K_1}{L_\lambda} + 1\right)} \tag{3}$$

where T is the TOA BT in Kelvin, L_λ represents the TOA spectral radiance, and K_1 and K_2 are the band-specific thermal conversion constants provided in the metadata. This transformation enables accurate retrieval of surface temperature variations by converting radiance into physical temperature values.

2.3 Estimation of Satellite Indices

The Combined Mangrove Recognition Index (CMRI: NDVI - NDWI) (Gupta et al., 2018) integrates outputs from the Normalized Difference Vegetation Index (NDVI: NIR – Red / NIR + Red) and Normalized Difference Water Index (NDWI: Green – NIR / Green + NIR) to enhance mangrove-specific vegetation classification. NDVI assesses chlorophyll content based on red and near-infrared (NIR) reflectance, while NDWI differentiates water-rich vegetation using NIR absorption (Bukowiecki et al., 2020). The pixel-wise subtraction of NDWI from NDVI enhances the distinction between mangroves and other land cover types with similar spectral signatures. CMRI thresho-ld modeling was applied to delineate mangrove extent within the study area. The threshold was manually determined through visual interpretation using Google Earth and reference studies. Since CMRI values vary seasonally and spatially, threshold selection was adjusted dynamically. Mangrove pixels exhibited higher CMRI values, while water bodies and open lands had lower values. For mangroves in arid environments, the threshold was adapted accordingly to ensure accurate separation from terrestrial vegetation. The extracted mangrove regions were further analyzed for LST variations.

The Normalized Difference Vegetation Index (NDVI) is a robust metric for mapping mangrove health by leveraging the differential absorption and reflectance of NIR and red light. NDVI values range from -1 to 1, where higher values indicate greater vegetation vigor (Monsef and Smith, 2017). Mangrove health was classified into four categories: Highly Stressed, Moderately Stressed, Healthy, and Very Healthy Vegetation using a scene-specific threshold approach with the help of QGIS software. The health classification provides insights into seasonal and environmental stressors impacting mangrove vitality, facilitating targeted conservation measures.

3. Results and Discussions

3.1 Mangrove Distribution and Seasonal Variability

A series of maps were generated to analyze the spatiotemporal distribution of mangroves in Abu Dhabi from 2013 to 2021. Three distinct months (April, August and December) were selected from each year to account for the seasonal variability of the mangrove health and distribution accurately. The extracted regions (marked in yellow), demonstrated stable spatial coverage but fluctuating density across seasons (Figure 3). Mangrove extent was notably reduced in August, indicating lower growth during peak summer conditions, while winter and spring exhibited increased coverage due to cooler temperatures and higher moisture availability. The mapping approach facilitated mangrove extraction but had limitations due to its reliance on manually set thresholds, affecting the precision of extent delineation. While useful for rapid detection, more accurate mapping requires field validation, high-resolution classification, and additional spectral indices (Gupta et al., 2018). Nevertheless, the extracted results remain valuable for correlation analyses with temperature variations and health indices. To assess temperature variations, surface temperature maps were generated (Figure 4). These maps confirmed expected seasonal fluctuations, with higher temperatures in summer (August) and lower temperatures in winter (December). Importantly, areas with mangrove presence consistently exhibited lower temperatures, suggesting a localized cooling effect through evapotranspiration and shading (Figure 5 and 4).

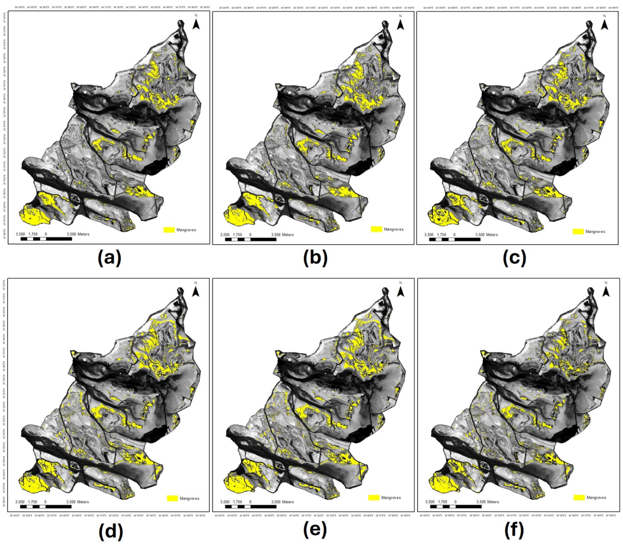

Figure 3. Spatiotemporal distribution in mangrove extent across the study region for 2013 and 2021. Panels (a–c) represent April, August, and December of 2013, while (d–f) show the corresponding months for 2021

Analysis showed that high-temperature zones correspond to highly stressed mangroves, while low-temperature zones align with healthier regions, reaffirming a negative correlation between temperature and vegetation health. A detailed assessment of the mangrove health index (Figure 6) categorizes the vegetation into highly stressed, moderately stressed, healthy, and very healthy, reflecting varying physiological conditions. The findings indicate that healthy areas peak in winter (December) and decline in summer (August), while highly stressed regions expand in summer and contract in winter. This suggests that tem-

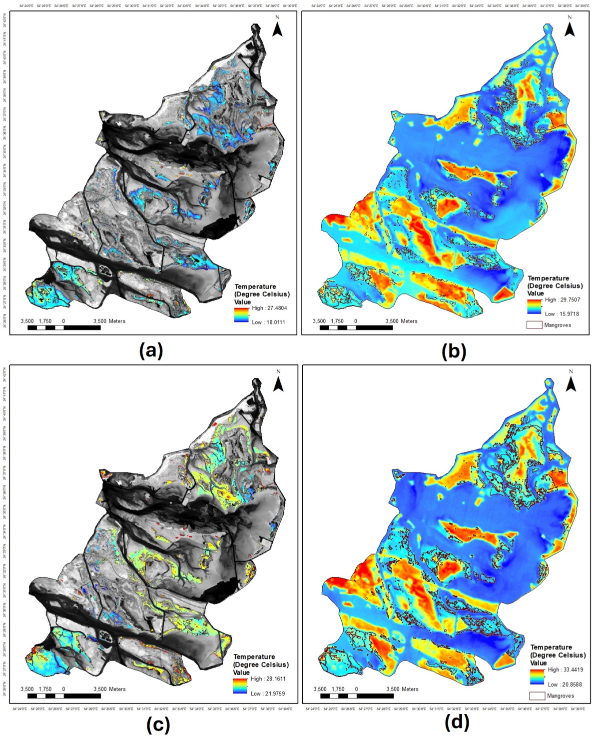

Figure 4. LST distribution over mangrove regions (a and c) and overall temperature variation across the study area (b and d) for December 2013 (top) and 2020 (bottom), highlighting temporal changes.

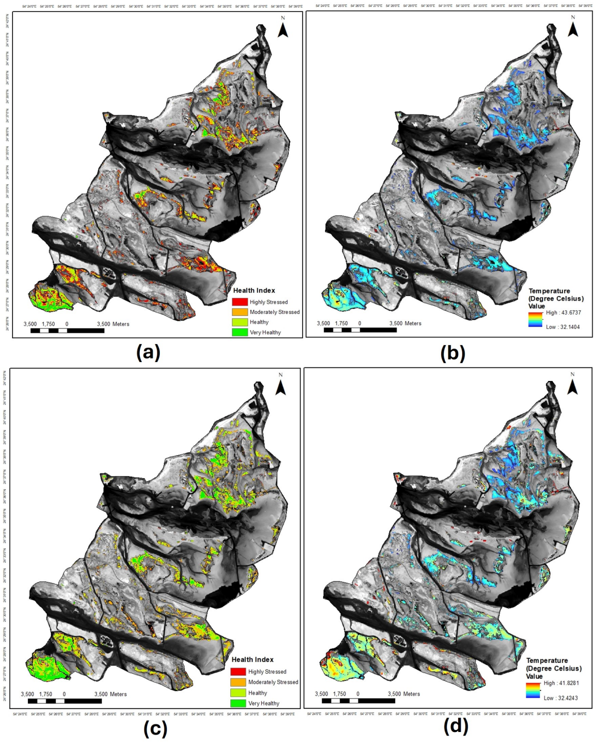

Figure 5. Mangrove health and LST distribution for August 2015 (top) and August 2019 (bottom). Panels (a, c) show mangrove health status from highly stressed to very healthy, while (b, d) depict corresponding temperature variations.

perature is a key driver of seasonal stress, with extreme heat exacerbating physiological strain (Gafoor et al., 2025). The observed patterns highlight the importance of continuous monitoring and adaptive conservation strategies to mitigate thermal stress impacts and support the long-term sustainability of coastal ecosystems. However, a notable 12% increase in total mangrove area by the end of 2021, compared to 2013, highlights the effectiveness of the ongoing monitoring and conservation strategies implemented over the years in the UAE (Elmahdy and Mohamed, 2013).

3.2 Temporal Trends in Mangrove Health and Temperature Correlation

A correlation analysis was conducted to assess the relationship between mangrove health and temperature across the study period, revealing a consistently negative correlation between the two variables (Figure 7). As temperatures rise, mangrove health tends to decline, while lower temperatures are associated with improved vegetation conditions. This inverse relationship suggests that thermal stress is a key factor influencing mangrove vitality, with excessive heat contributing to physiological strain and reduced productivity. The analysis of mangrove extent over time reveals noticeable seasonal variations, with fluctuations in coverage influenced by environmental conditions (Figure 8). However, no distinct long-term trend was observed, indicating that while seasonal dynamics are evident, external factors such as conservation efforts, tidal influences, and classification uncertainties may contribute to variability in estimated mangrove coverage. Despite being an effective tool for rapid detection, the CMRI method relies on manually set thresholds, which may have introduced classification inconsistencies, leading to potential misclassification or omission of certain mangrove areas

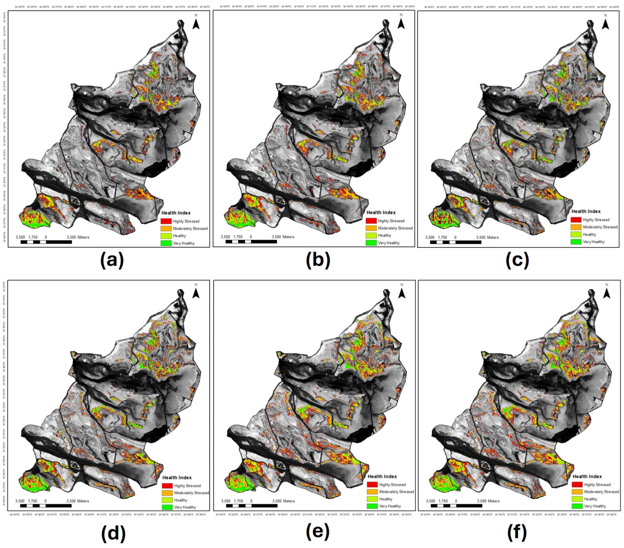

Figure 6. The classification of mangrove health extent across three distinct seasons in 2013 (top) and 2020 (bottom) is depicted, showing variations for April (a and d), August (b and e), and December (c and f)

(Gupta et al., 2018). These limitations highlight the need for enhanced classification techniques and higher-resolution datasets to improve the accuracy of mangrove extent monitoring.

Similarly, NDVI exhibits distinct seasonal fluctuations, with higher values observed during winter and a notable decline in summer. This pattern further underscores the influence of tem-

https://doi.org/10.5194/isprs-archives-XLVIII-G-2025-3-2025 | © Author(s) 2025. CC BY 4.0 License.

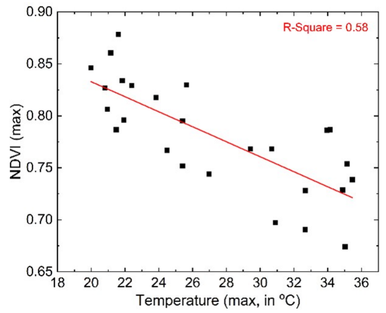

Figure 7. Delineation of the inverse relationship of the NDVI with increasing temperature

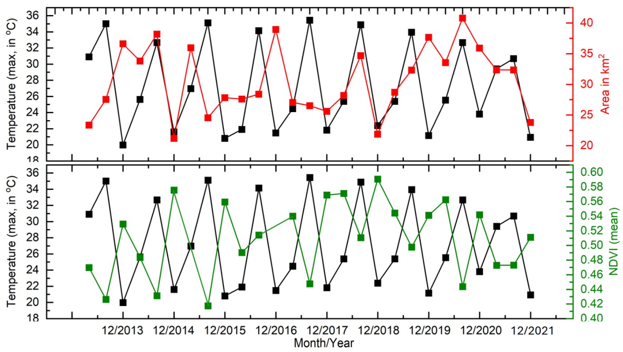

Figure 8. Temporal analysis illustrating the relationship between (a) LST vs. Mangrove extent and (b) LST vs. NDVI.

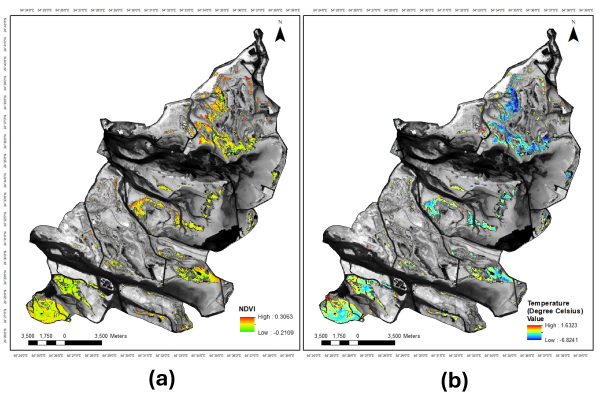

Figure 9. Spatial anomalies in (a) NDVI and (b) LST, quantified as the difference between 2021 and 2013 values in August

perature variations on mangrove ecosystems, where cooler conditions support healthier vegetation, while extreme summer temperatures contribute to increased physiological stress. Although both mangrove extent and NDVI exhibit seasonal fluctuations, their mean values show a gradual increasing trend over the years. Anomalous analysis of NDVI and LST between 2013 and 2021 reveals a notable enhancement in mangrove health over this period, accompanied by a localized reduction in temperature in regions with thriving mangroves (Figure 9).

4. Conclusion

This study examined the seasonal and long-term dynamics of mangrove ecosystems in Abu Dhabi using remote sensing techniques over a period starting from 2013 to 2021. The analysis integrated satellite-derived indices with land surface temperature data to assess mangrove extent, health, and thermal stress. The results demonstrated that coverage remains spatially stable but exhibits significant seasonal variations in density, with reduced extents in summer and peak growth during winter and spring. The negative correlation observed between temperature and health further highlights the impact of thermal stress, where elevated temperatures contribute to vegetation decline, while cooler conditions promote vitality. Despite the limitations associated with thresholding, the extracted regions provided valuable insights into broader ecological trends. The statistical analysis of vegetation trends revealed a progressive increase in health and density over the years, corroborating the effectiveness of ongoing conservation initiatives. However, the seasonal variations underscore the need for continuous monitoring and adaptive management strategies to mitigate climate-induced stress.

The findings of this study emphasize the importance of leveraging remote sensing for long-term monitoring, offering a scalable and cost-effective approach to track changes in vegetation health and environmental conditions. Future work should integrate higher-resolution datasets and advanced classification techniques to enhance the precision of mapping. Additionally, incorporating field-based validation will improve the accuracy of health assessments and support sustainable conservation efforts in arid coastal environments.

References

Al Shehhi, M. R., Gherboudj, I., Ghedira, H., 2017. *In situ* spectral response of the Arabian Gulf and Sea of Oman coastal waters to bio-optical properties. *Journal of Photochemistry and Photobiology B: Biology*, 175, 235–243.

Al Shehhi, M. R., Kaya, A., 2021. Time series and neural network to forecast water quality parameters using satellite data. *Continental Shelf Research*, 231, 104612.

Al-Shehhi, M. R., Song, H., Scott, J., Marshall, J., 2021. Water mass transformation and overturning circulation in the Arabian Gulf. *Journal of Physical Oceanography*, 51(11), 3513–3527. https://journals.ametsoc.org/view/journals/phoc/51/11/JPO-D-20-0249.1.xml.

Alongi, D. M., 2015. The Impact of Climate Change on Mangrove Forests. *Current Climate Change Reports*, 1(1), 30–39. https://doi.org/10.1007/s40641-015-0002-x.

Amrousi, M. E., Paleologos, E. K., Elhakeem, M., 2024. Waterfront Developments and Public Space. *International Review for Spatial Planning and Sustainable Development*, 12(1), 44–58.

Asmara, T. M., Saraswati, R., Hernina, R., 2021. Distribution and area changes of mangroves with remote sensing technology in Perancak Estuary, Jembrana, Bali. *Journal of Physics: Conference Series*, 1725(1), 012069. https://dx.doi.org/10.1088/1742-6596/1725/1/012069. Publisher: IOP Publishing.

Baloloy, A. B., Blanco, A. C., Sta. Ana, R. R. C., Nadaoka, K., 2020. Development and application of a new mangrove vegetation index (MVI) for rapid and accurate mangrove mapping. *ISPRS Journal of Photogrammetry and Remote Sensing*, 166, 95–117.

Bukowiecki, J., Rose, T., Ehlers, R., Kage, H., 2020. High-Throughput Prediction of Whole Season Green Area Index in Winter Wheat With an Airborne Multispectral Sensor. *Frontiers in Plant Science*, 10. Publisher: Frontiers.

Congedo, L., 2021. Semi-Automatic Classification Plugin: A Python tool for the download and processing of remote sensing images in QGIS. *The Journal of Open Source Software*, 6, 3172.

Elmahdy, S. I., Mohamed, M. M., 2013. Change detection and mapping of mangrove using multitemporal remote sensing data; a case study of Abu Dhabi, UAE. *Journal of Geomatics*, 7.

Faridah-Hanum, I., Yusoff, F. M., Fitrianto, A., Ainuddin, N. A., Gandaseca, S., Zaiton, S., Norizah, K., Nurhidayu, S., Roslan, M. K., Hakeem, K. R., Shamsuddin, I., Adnan, I., Awang Noor, A. G., Balqis, A. R. S., Rhyma, P. P., Siti Aminah, I., Hilaluddin, F., Fatin, R., Harun, N. Z. N., 2019. Development of a comprehensive mangrove quality index (*MQI*) in Matang Mangrove: Assessing mangrove ecosystem health. *Ecological Indicators*, 102, 103–117.

Gafoor, F. A., Lathif, S. A., Addad, Y., Shehhi, S. A., Shehhi, M. R. A., 2025. High-resolution monitoring and modelling of thermal plumes from nuclear power plants in the Arabian Gulf. *Active and Passive Remote Sensing of Oceans, Seas, and Lakes*, 13264, SPIE, 71–75.

Gandhi, S., Jones, T. G., 2019. Identifying Mangrove Deforestation Hotspots in South Asia, Southeast Asia and Asia-Pacific. *Remote Sensing*, 11(6), 728. https://www.mdpi.com/2072-4292/11/6/728. Number: 6 Publisher: Multidisciplinary Digital Publishing Institute.

Godoy, M. D. P., Lacerda, L. D. d., 2015. Mangroves Response to Climate Change: A Review of Recent Findings on Mangrove Extension and Distribution. *Anais da Academia Brasileira de Ciências*, 87, 651–667. Publisher: Academia Brasileira de Ciências.

Gupta, K., Mukhopadhyay, A., Giri, S., Chanda, A., Datta Majumdar, S., Samanta, S., Mitra, D., Samal, R. N., Pattnaik, A. K., Hazra, S., 2018. An index for discrimination of mangroves from non-mangroves using LANDSAT 8 OLI imagery. *MethodsX*, 5, 1129–1139.

Lathif, S. A., Al Shehhi, M. R., 2025. Sensitivity Assessment of Atmospheric Corrections for Clear and Moderately Turbid Optical Waters. *IEEE Journal of Selected Topics in Applied Earth Observations and Remote Sensing*, 18, 1174–1195. https://ieeexplore.ieee.org/document/10745643. Conference Name: IEEE Journal of Selected Topics in Applied Earth Observations and Remote Sensing.

Monsef, H. A.-E., Smith, S. E., 2017. A new approach for estimating mangrove canopy cover using Landsat 8 imagery. *Computers and Electronics in Agriculture*, 135, 183–194.

Nyanga, C., 2020. The Role of Mangroves Forests in Decarbonizing the Atmosphere. *Carbon-Based Material for Environmental Protection and Remediation*, IntechOpen.

Osland, M. J., Feher, L. C., López-Portillo, J., Day, R. H., Suman, D. O., Guzmán Menéndez, J. M., Rivera-Monroy, V. H., 2018. Mangrove forests in a rapidly changing world: Global change impacts and conservation opportunities along the Gulf of Mexico coast. *Estuarine, Coastal and Shelf Science*, 214, 120–140.

Pagkalinawan, H., 2015. A. Mangrove Forest Mapping using LandSat 8 Imageries. *State of the Mangrove Summit: Northwestern Luzon Proceedings*, 60.

Paleologos, E. K., Welling, B. A., Amrousi, M. E., Masalmeh, H. A., 2019. Coastal development and mangroves in Abu Dhabi, UAE. *IOP Conference Series: Earth and Environmental Science*, 344(1), 012020. Publisher: IOP Publishing.

Pham, T. D., Yokoya, N., Bui, D. T., Yoshino, K., Friess, D. A., 2019. Remote Sensing Approaches for Monitoring Mangrove Species, Structure, and Biomass: Opportunities and Challenges. *Remote Sensing*, 11(3), 230. https://www.mdpi.com/2072-4292/11/3/230. Number: 3 Publisher: Multidisciplinary Digital Publishing Institute.

Shehhi, M. R. A., Nelson, D., Alkhori, R. R., Alshihi, R., Salehi-Ashtiani, K., 2020. Characterizing Algal blooms in a shallow and a deep channel over a decade (2008-2018). arXiv:2003.05694 [q-bio].

Using the USGS Landsat Level-1 Data Product | U.S. Geological Survey, 2024.

Worthington, T. A., Andradi-Brown, D. A., Bhargava, R., Buelow, C., Bunting, P., Duncan, C., Fatoyinbo, L., Friess, D. A., Goldberg, L., Hilarides, L., Lagomasino, D., Landis, E., Longley-Wood, K., Lovelock, C. E., Murray, N. J., Narayan, S., Rosenqvist, A., Sievers, M., Simard, M., Thomas, N., Eijk, P. v., Zganjar, C., Spalding, M., 2020. Harnessing Big Data to Support the Conservation and Rehabilitation of Mangrove Forests Globally. *One Earth*, 2(5), 429–443. Publisher: Elsevier.

Yousif, O. M., Sen, S., 2020. Reintroduction of red mangrove Rhizophora mucronata in Abu Dhabi Emirate, United Arab Emirates. *World Journal of Advanced Research and Reviews*, 7(2), 210–217. Last Modified: 2021-06-17T17:03+05:30 Publisher: World Journal of Advanced Research and Reviews.